

Carranza-Torres, C. (2004). Elasto-plastic solution of tunnel problems using the generalized form of the Hoek-Brown failure criterion. Proceedings of the ISRM SINOROCK 2004 Symposium China, May 2004. Edited by J.A. Hudson and F. Xia-Ting. *International Journal of Rock Mechanics and Mining Sciences* 41(3), 480–481.

ELASTO-PLASTIC SOLUTION OF TUNNEL PROBLEMS USING THE GENERALIZED FORM OF THE HOEK-BROWN FAILURE CRITERION

C. Carranza-Torres¹

¹) Itasca Consulting Group Inc., Minnesota, USA

cct@itascacg.com

Abstract: The Hoek-Brown failure criterion is a semi-empirical method widely used in the estimation of shear strength of rock. Among other parameters involved in this criterion, the coefficient a dictates whether the criterion applies to intact rock or rock masses ($a = 0.5$ for intact rock and $a > 0.5$ for rock masses). Most of the existing elasto-plastic solutions for tunnel problems in Hoek-Brown media consider an intact rock (i.e., $a = 0.5$). This is not only due to historical reasons (the failure criterion was originally developed for intact rock), but also due to the mathematical difficulties of deriving neat, closed-form expressions for the general case in which $a \geq 0.5$. This paper presents a rigorous, elasto-plastic solution for the axi-symmetrical problem of excavating a circular tunnel in generalized Hoek-Brown material ($a \geq 0.5$). The solution is obtained by re-writing the generalized Hoek-Brown failure criterion in terms of transformed stress quantities. Application of the transformation rule described in this paper to elasto-plastic problems of excavations in generalized Hoek-Brown materials is shown to bring significant advantages in the interpretation and extrapolation of results obtained with analytical and numerical methods.

Keywords: Rock strength, Hoek-Brown criterion, Tunnel solution, Plasticity, Elasticity.

1. INTRODUCTION

The Hoek-Brown failure criterion was introduced in the early eighties to describe the shear strength of intact rock as measured in triaxial tests (Hoek & Brown 1980). The failure criterion for intact rock defines the combination of major and minor principal stresses (σ_1 and σ_3) at failure to be

$$\sigma_1 = \sigma_3 + \sigma_{ci} \sqrt{m_i \frac{\sigma_3}{\sigma_{ci}} + 1} \quad (1)$$

In the equation above, σ_{ci} is the unconfined compressive strength of the rock and the coefficient m_i is a parameter that depends on the type of rock (normally $5 \leq m_i \leq 40$). Both parameters, σ_{ci} and m_i , can be determined from regression analysis of triaxial test results (Hoek & Brown 1980; Hoek, Kaiser, & Bawden 1995).

The Hoek-Brown failure criterion was later extended to define the shear strength of rock masses. This form of the failure criterion, that is normally referred to as the *generalized* Hoek-Brown failure criterion, is

$$\sigma_1 = \sigma_3 + \sigma_{ci} \left(m_b \frac{\sigma_3}{\sigma_{ci}} + s \right)^a \quad (2)$$

The coefficients m_b , s and a in equation (2) are semi-empirical parameters that characterize the rock mass.

In practice, these parameters are computed based on an empirical index called the Geological Strength Index or GSI. This index lies in range 0 to 100 and can be quantified from charts based on the quality of the rock structure and the condition of the rock surfaces (Hoek & Brown 1997; Hoek, Marinos, & Benissi 1998; Marinos & Hoek 2000).

In the latest update of the Hoek-Brown failure criterion, the relationship between the coefficients m_b , s and a in equation (2) and the GSI is as follows (Hoek, Carranza-Torres, & Corkum 2002)

$$m_b = m_i \exp\left(\frac{\text{GSI} - 100}{28 - 14D}\right) \quad (3)$$

$$s = \exp\left(\frac{\text{GSI} - 100}{9 - 3D}\right) \quad (4)$$

$$a = \frac{1}{2} + \frac{1}{6} \left(e^{-\text{GSI}/15} - e^{-20/3} \right) \quad (5)$$

In equations (3) and (4) D is a factor that depends on the degree of disturbance to which the rock has been subjected to blast damage and stress relaxation. This factor varies between 0 and 1. [The computer code *Roclab* (Rocscience 2002), which can be downloaded freely from www.rocscience.com, guides the user through the selection of appropriate values of

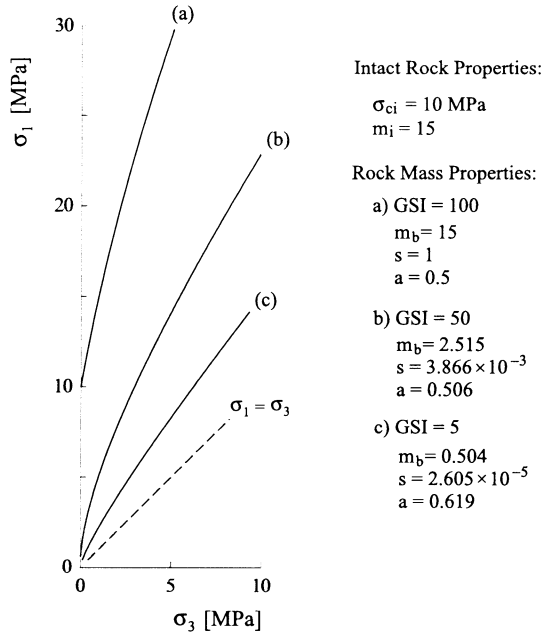


Figure 1. Hoek-Brown failure criterion for intact rock (curve a) and rock masses with decreasing values of GSI (curves b and c).

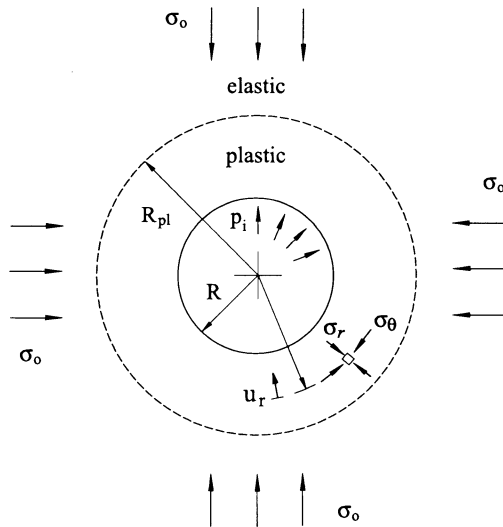


Figure 2. The problem of excavating a circular tunnel in an elasto-plastic material subject to uniform loading.

GSI, D and other significant Hoek-Brown parameters in practical situations.]

It is worth noting that the failure criterion for intact rock (equation 1) can be recovered from the failure criterion for rock masses (equation 2) by making $m_b = m_i$, $s = 1$ and $a = 0.5$. Figure 1 illustrates

the relationship between the shear strength of intact rock and rock masses. Curve (a) represents the shear strength of intact rock (that corresponds to a value of $GSI=100$). Curves (b) and (c) represent the failure criterion for decreasing values of GSI, as indicated by the values on the right side of the figure. Note that by decreasing the quality of the rock mass (i.e., the value of GSI), the Hoek-Brown parabola is ‘flattened’ towards the lowest limit of shear strength $\sigma_1 = \sigma_3$.

A fundamental problem in rock engineering involves the evaluation of the failure zone and convergence of the wall of a circular opening (see Figure 2). This problem has applications in the determination of stability of boreholes and underground openings, and the design of tunnel liners according to the Convergence-Confinement method. In the simplest case, both the internal pressure acting on the walls of the tunnel and the initial stresses in the surrounding rock mass can be considered to be uniform. Under these conditions, the failure zone is circular and the convergence of the tunnel wall is also uniform.

Analytical solutions for the problem in Figure 2, in which the material obeys the Hoek-Brown failure criterion, have been reported in the literature (Brown, Bray, Ladanyi, & Hoek 1983; Wang 1996; Sharan 2003). Almost all of these solutions consider that the material satisfies the criterion for intact rock (i.e., $a = 0.5$, as in equation 1), rather than the generalized criterion for rock masses (i.e., $a \geq 0.5$, as in equation 2). The reasons are in part historical, but are also due to the fact that neat, closed-form expressions for the tunnel problem can not be easily obtained when $a > 0.5$.

In the following sections a rigorous, neat solution for the problem in Figure 2, that satisfies the generalized Hoek-Brown criterion (equation 2), is presented. The solution is based on a self-similar formulation for tunnel problems satisfying the Hoek-Brown failure criterion for intact rock (equation 1), described in Carranza-Torres & Fairhurst (1999).

The solution to be discussed here relies on a transformation rule for stresses that simplifies significantly the formulation of elasto-plastic problems involving the generalized Hoek-Brown failure criterion. This transformation rule is described next.

2. TRANSFORMATION OF THE HOEK-BROWN FAILURE CRITERION

Londe (1988) showed that the Hoek-Brown failure criterion (equation 1) can be compactly written

as follows

$$S_1 = S_3 + \sqrt{S_3} \quad (6)$$

where S_1 and S_3 represent principal stresses σ_1 and σ_3 , transformed as follows

$$S_1 = \frac{\sigma_1}{m_i \sigma_{ci}} + \frac{1}{m_i^2} \quad (7)$$

$$S_3 = \frac{\sigma_3}{m_i \sigma_{ci}} + \frac{1}{m_i^2} \quad (8)$$

The transformation rule proposed by Londe can be naturally extended to the generalized Hoek-Brown failure criterion (equation 2) by transforming the stresses according to the following rule

$$S_1 = \frac{\sigma_1}{m_b^{(1-a)/a} \sigma_{ci}} + \frac{s}{m_b^{1/a}} \quad (9)$$

$$S_3 = \frac{\sigma_3}{m_b^{(1-a)/a} \sigma_{ci}} + \frac{s}{m_b^{1/a}} \quad (10)$$

In view of equations (9) and (10), the failure criterion for rock masses (equation 2) can now be simply written as

$$S_1 = S_3 + \mu S_3^a \quad (11)$$

where the parameter μ is

$$\mu = m_b^{(2a-1)/a} \quad (12)$$

Note that when $a = 0.5$ (the case analyzed by Londe), the coefficient μ in equation (12) is one, and therefore expressions (11) and (6) are identical—also, for this case, expressions (9) and (10) reduce to equations (7) and (8) respectively.

The generality obtained by applying the transformed Hoek-Brown failure criterion for rock masses (equation 11) can be illustrated by a simple numerical exercise.

Figure 3a represents the failure state for 2,000 randomly generated pairs of stresses (σ_1 and σ_3), which are computed using the failure criterion for rock masses. In practical terms, the dots in the diagram represent 2,000 different, arbitrary cases of failure according to the generalized Hoek-Brown failure criterion given by equation (2). The cases represented in Figure 3a are chosen from a (uniform) distribution of randomly generated parameters lying in the ranges indicated in Table 1.

The random nature of the cases is clearly reflected in Figure 3a. No evident ‘order’ appears to exist in the values of predicted shear strength.

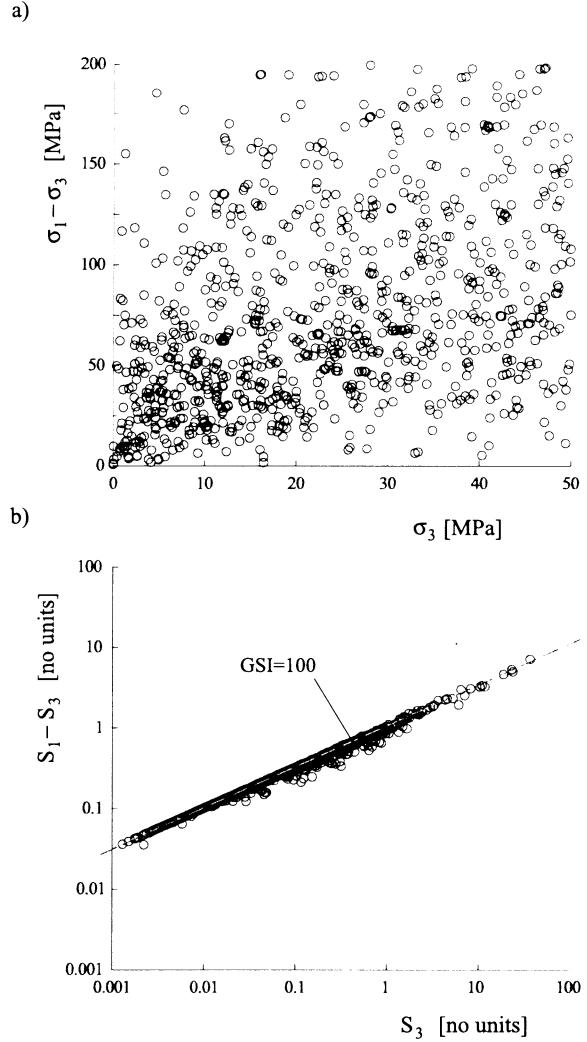


Figure 3. Shear strength predicted with the generalized Hoek-Brown failure criterion for 2,000 random cases. Strength is represented in terms of a) actual and b) transformed stresses.

Figure 3b shows the same pairs representing failure in Figure 3a, after the stresses have been transformed according to expressions (9) and (10), using the corresponding values of σ_{ci} , m_b , s and a as in Table 1. In this new representation, the points describing possible failure states are clearly concentrated along a line, that in the log-log representation of Figure 3b obeys equation (11) with the random values of coefficients μ and a . It can also be observed that most of the points in Figure 3b lie below a dashed straight line. This line, that corresponds to the highest quality of rock mass (GSI = 100), obeys the transformed failure criterion proposed by Londe (equation 6).

Table 1. Characteristics of the (uniform) randomly generated series of parameters for the analysis of Hoek-Brown shear strength.

Variable	Minimum	Maximum
σ_{ci} [MPa]	0.01	200
m_i [no units]	5	35
GSI [no units]	5	100
σ_3 [MPa]	0	50

Note: The values of m_b , s and a were computed from the values of GSI above using equations (3), (4) and (5) respectively (a factor $D = 0$ was considered).

The simple numerical exercise just described suggests that the transformation rule for stresses (equations 9 and 10) can also be applied to solve problems in which the generalized Hoek-Brown failure criterion applies. By doing so, one can expect that results expressed in terms of transformed stresses will reveal the form of the fundamental relationships among variables in the problem. In practical terms, this would imply that the results obtained for some parameters in the problem could be used to extrapolate results for other parameters that are not actually solved. This concept will be illustrated in Section 4. First, the elasto-plastic solution of the problem in Figure 2 for generalized Hoek-Brown material will be presented.

3. SOLUTION OF A CIRCULAR TUNNEL EXCAVATED IN GENERALIZED HOEK-BROWN MATERIAL ($a \geq 0.5$)

The solution presented in this section takes advantage of the properties of self-similarity of the problem in Figure 2 to determine the field quantities, radial and hoop stresses and radial displacement, in the plastic region $r \leq R_{pl}$. This approach has been discussed in detail in Carranza-Torres & Fairhurst (1999). Here, only the final expressions will be presented (the reader interested in the details of the formulation is referred to the publication mentioned above). A validation example, including a comparison of the results with the finite difference code *FLAC* (Itasca Consulting Group, Inc. 2000) and a computer spreadsheet implementing the solution, are presented separately as Appendices A and B, respectively.

The generalized Hoek-Brown material surrounding the opening in Figure 2 will be considered to

allow for softening of shear strength. Two failure envelopes will be considered; one for the *peak* strength (curve 1 in Figure 4) and one for the *residual* strength (curve 2). The Hoek-Brown parameters defining the *peak* failure envelope (curve 1) are σ_{ci} , m_b , s and a . The parameters defining the *residual* failure envelope (curve 2) will be identified with the symbol ‘ \sim ’—i.e., they are $\tilde{\sigma}_{ci}$, \tilde{m}_b , \tilde{s} and \tilde{a} .

[Note that perfectly-plastic behavior for the generalized Hoek-Brown material can also be considered in the solution. This simply requires assuming residual and peak parameters to be the same.]

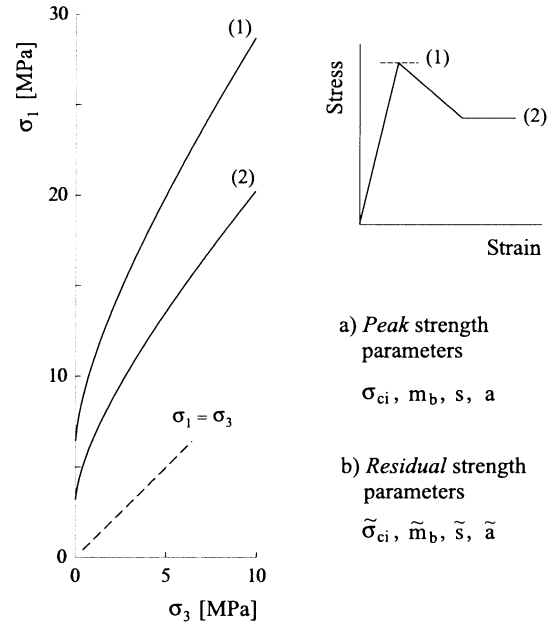


Figure 4. Peak and residual failure envelopes considered for the generalized Hoek-Brown failure criterion for the problem in Figure 2.

The stress quantities involved in the problem of Figure 2 will be transformed using the Hoek-Brown parameters as explained in Section 2. Capital letters will be used to indicate transformed stresses and the symbol ‘ \sim ’ will indicate transformation with respect to the residual parameters.

For example, the following are transformed stresses using *peak* Hoek-Brown properties:

$$S_o = \frac{\sigma_o}{m_b^{(1-a)/a} \sigma_{ci}} + \frac{s}{m_b^{1/a}} \quad (13)$$

$$P_i = \frac{p_i}{m_b^{(1-a)/a} \sigma_{ci}} + \frac{s}{m_b^{1/a}} \quad (14)$$

$$P_i^{cr} = \frac{p_i^{cr}}{m_b^{(1-a)/a} \sigma_{ci}} + \frac{s}{m_b^{1/a}} \quad (15)$$

The following are transformed stresses using *residual* Hoek-Brown properties:

$$\tilde{S}_o = \frac{\sigma_o}{\tilde{m}_b^{(1-\tilde{a})/\tilde{a}} \tilde{\sigma}_{ci}} + \frac{\tilde{s}}{\tilde{m}_b^{1/\tilde{a}}} \quad (16)$$

$$\tilde{P}_i = \frac{p_i}{\tilde{m}_b^{(1-\tilde{a})/\tilde{a}} \tilde{\sigma}_{ci}} + \frac{\tilde{s}}{\tilde{m}_b^{1/\tilde{a}}} \quad (17)$$

$$\tilde{P}_i^{cr} = \frac{p_i^{cr}}{\tilde{m}_b^{(1-\tilde{a})/\tilde{a}} \tilde{\sigma}_{ci}} + \frac{\tilde{s}}{\tilde{m}_b^{1/\tilde{a}}} \quad (18)$$

In the equations above, σ_o and p_i are the far-field stress and the internal pressure, respectively (see Figure 2), while p_i^{cr} is the internal pressure below which the plastic zone of extent R_{pl} develops.

A parameter $\tilde{\mu}$, similar to the one introduced in equation (12) but computed in terms of residual properties, will also be considered, i.e.,

$$\tilde{\mu} = \tilde{m}_b^{(2\tilde{a}-1)/\tilde{a}} \quad (19)$$

Following the similarity formulation in Carranza-Torres & Fairhurst (1999), the critical internal pressure P_i^{cr} (transformed using peak properties) can be computed from the following transcendental equation

$$\mu P_i^{cr a} + 2P_i^{cr} - 2S_o = 0 \quad (20)$$

A closed-form (exact) solution that satisfies the equation above can be found only when $a = 0.5$; for this case

$$P_i^{cr} = \left[\frac{1 - \sqrt{1 + 16S_o}}{4} \right]^2 \quad (21)$$

Numerical methods, like the Newton-Raphson method, can be applied to approximate the exact solution to equation (20) (Press, Flannery, Teukolsky, & Vetterling 1994).

[Sofianos (2003) proposed an expression to compute the value of critical internal pressure satisfying equation (20). It should be noted that his expression gives a reasonable approximation to the solution (for the range of Hoek-Brown parameters normally used in practice), but does not give the actual (exact) solution to the equation.]

Once the transformed value of P_i^{cr} has been determined from equation (20), the actual value of internal pressure p_i^{cr} can be found from the inversion of equation (15), i.e.,

$$p_i^{cr} = \left[P_i^{cr} - \frac{s}{m_b^{1/a}} \right] m_b^{(1-a)/a} \sigma_{ci} \quad (22)$$

In agreement with the similarity formulation mentioned earlier, the extent of the plastic zone R_{pl} is computed with the following expression

$$\frac{R_{pl}}{R} = \exp \left[\frac{\tilde{P}_i^{cr} 1-\tilde{a} - \tilde{P}_i 1-\tilde{a}}{(1-\tilde{a}) \tilde{\mu}} \right] \quad (23)$$

[Note that in the equation above the transformed critical internal pressure is not the same as in equation (20). In equation (20), the critical internal pressure is transformed using *peak* parameters, while in equation (23), it is transformed using *residual* parameters].

From the similarity solution, the distribution of transformed radial stress in the plastic region is found to be

$$\tilde{S}_r = \left[\tilde{P}_i^{cr} 1-\tilde{a} + (1-\tilde{a}) \tilde{\mu} \ln \left(\frac{r}{R_{pl}} \right) \right]^{1-\tilde{a}} \quad (24)$$

and the distribution of transformed hoop stress,

$$\tilde{S}_\theta = \tilde{S}_r + \tilde{\mu} \tilde{S}_r^{\tilde{a}} \quad (25)$$

In view of the transformations (16) through (18), the actual values of radial and hoop stresses are obtained, respectively, as follows

$$\sigma_r = \left[\tilde{S}_r - \frac{\tilde{s}}{\tilde{m}_b^{1/\tilde{a}}} \right] \tilde{m}_b^{(1-\tilde{a})/\tilde{a}} \tilde{\sigma}_{ci} \quad (26)$$

$$\sigma_\theta = \left[\tilde{S}_\theta - \frac{\tilde{s}}{\tilde{m}_b^{1/\tilde{a}}} \right] \tilde{m}_b^{(1-\tilde{a})/\tilde{a}} \tilde{\sigma}_{ci} \quad (27)$$

Determination of the radial displacements in the plastic zone requires solving the following differential equation,

$$\rho^2 \frac{du_r^2}{d^2\rho} - A_1 \rho \frac{du_r}{d\rho} + A_1 u_r - \frac{R_{pl}}{2\tilde{G}} \rho^2 \left[A_2 \frac{d\tilde{S}_r}{d\rho} - A_3 \frac{d\tilde{S}_\theta}{d\rho} \right] = 0 \quad (28)$$

In the equation above, the independent variable ρ is

$$\rho = \frac{r}{R_{pl}} \quad (29)$$

The quantity \tilde{G} is the shear modulus of the material normalized with respect to residual Hoek-Brown parameters, as follows,

$$\tilde{G} = \frac{G}{\tilde{m}_b^{(1-\tilde{a})/\tilde{a}} \tilde{\sigma}_{ci}} \quad (30)$$

The quantities $d\tilde{S}_r/d\rho$ and $d\tilde{S}_\theta/d\rho$ represent the first derivative of the transformed stresses \tilde{S}_r and \tilde{S}_θ (equations 24 and 25), with respect to the independent variables ρ , i.e.,

$$\frac{d\tilde{S}_r}{d\rho} = \frac{\tilde{\mu}}{\rho} \tilde{S}_r^{\tilde{a}} \quad (31)$$

$$\frac{d\tilde{S}_\theta}{d\rho} = \left(1 + \tilde{a}\tilde{\mu} \tilde{S}_r^{\tilde{a}-1}\right) \frac{d\tilde{S}_r}{d\rho} \quad (32)$$

The coefficients A_1 , A_2 and A_3 in equation (28) depend on the Poisson's ratio ν and the flow rule considered for the material.

For a *linear* flow rule, the coefficients are computed as

$$A_1 = -K_\psi \quad (33)$$

$$A_2 = 1 - \nu - \nu K_\psi \quad (34)$$

$$A_3 = \nu - (1 - \nu)K_\psi \quad (35)$$

where the coefficient K_ψ depends on the dilation angle ψ , according to the following expression

$$K_\psi = \frac{1 + \sin \psi}{1 - \sin \psi} \quad (36)$$

For an *associated* flow-rule (i.e., a flow rule derived from a potential that has the same form as the failure surface), the coefficients A_1 , A_2 and A_3 are computed as

$$A_1(\rho) = -\frac{d\sigma_r}{d\rho} \quad (37)$$

$$A_2(\rho) = 1 - \nu - \nu \frac{d\sigma_r}{d\rho} \quad (38)$$

$$A_3(\rho) = \nu - (1 - \nu) \frac{d\sigma_r}{d\rho} \quad (39)$$

The boundary conditions needed to integrate the differential equation (28) are the radial displacement and the first derivative with respect to the variable ρ at the elasto-plastic interface (i.e., at $\rho = 1$). These expressions can be found from the condition of compatibility of displacements of the plastic and elastic regions, and result to be

$$u_r(1) = \frac{R_{pl}}{2\tilde{G}} \left(\tilde{S}_o - \tilde{P}_i^{cr}\right) \quad (40)$$

$$u'_r(1) = A_1 u_r(1) \quad (41)$$

$$+ \frac{R_{pl}}{2\tilde{G}} [1 - \nu(1 - A_1)] \left[\tilde{P}_i^{cr} - \tilde{S}_o\right] \\ - \frac{R_{pl}}{2\tilde{G}} [A_1 + \nu(1 - A_1)] \left[\tilde{P}_i^{cr} + \tilde{\mu} \tilde{P}_i^{cr\tilde{a}} - \tilde{S}_o\right]$$

The differential equation (28) can be integrated using numerical techniques, such as the Runge-Kutta method (Press, Flannery, Teukolsky, & Vetterling 1994). A closed-form solution is only possible when $a = 0.5$ and the flow rule is linear—i.e., when the coefficients A_1 , A_2 and A_3 are given by equations (33), (34) and (35) respectively; in this case, the solution is

$$u_r = \frac{1}{1 - A_1} (\rho^{A_1} - A_1 \rho) u_r(1) \\ + \frac{1}{1 - A_1} (\rho - \rho^{A_1}) u'_r(1) \\ + \frac{R_{pl}}{2\tilde{G}} \frac{1}{4} \frac{A_2 - A_3}{1 - A_1} \rho (\ln \rho)^2 \\ + \frac{R_{pl}}{2\tilde{G}} \left[\frac{A_2 - A_3}{(1 - A_1)^2} \sqrt{\tilde{P}_i^{cr}} - \frac{1}{2} \frac{A_2 - A_1 A_3}{(1 - A_1)^3} \right] \\ \times [\rho^{A_1} - \rho + (1 - A_1) \rho \ln \rho] \quad (42)$$

For the elastic-region $r \geq R_{pl}$, the solution is known already from Lamé's solution. Using the same notation as in the solution for the plastic region, the transformed radial and hoop stresses and the radial displacement in the elastic region are given by the following expressions

$$\tilde{S}_r = \tilde{S}_o - \left(\tilde{S}_o - \tilde{P}_i^{cr}\right) \left(\frac{R_{pl}}{r}\right)^2 \quad (43)$$

$$\tilde{S}_\theta = \tilde{S}_o + \left(\tilde{S}_o - \tilde{P}_i^{cr}\right) \left(\frac{R_{pl}}{r}\right)^2 \quad (44)$$

$$u_r = \frac{\tilde{S}_o - \tilde{P}_i^{cr}}{2\tilde{G}} \frac{R_{pl}^2}{r} \quad (45)$$

The solution for the plastic and elastic regions presented in this section is validated with an application example in Appendix A. The results for this validation problem are obtained with a computer spreadsheet that implements the solution discussed above. The spreadsheet and the cell formulae are presented in Appendix B.

4. DIMENSIONLESS REPRESENTATION OF TUNNEL RESULTS

As mentioned in Section 2, the use of the transformation rule for stresses in the solution of tunnel problems can bring considerable advantages in the interpretation of results. To illustrate this, we will apply the elasto-plastic solution in Section 2 to solve randomly generated cases of tunnel excavation problems. The material properties will be the

same (randomly generated) Hoek-Brown parameters listed in Table 1 (see also Figure 3). To simplify the analysis, we will assume that the material behaves in a perfectly plastic manner (peak and residual properties will be assumed to be the same) and that the tunnels are unsupported (i.e., $p_i = 0$). To complement the random material parameters (Table 1), we will also consider 2,000 (uniform) randomly generated values of far-field stresses σ_o , in the arbitrary range of 0 through 50 MPa. Young's modulus values will be computed using the modified semi-empirical relationships by Serafim and Pereira (Serafim & Pereira 1983), described in Hoek, Carranza-Torres, & Corkum (2002), as a function of the randomly generated values of σ_{ci} (see Table 1).

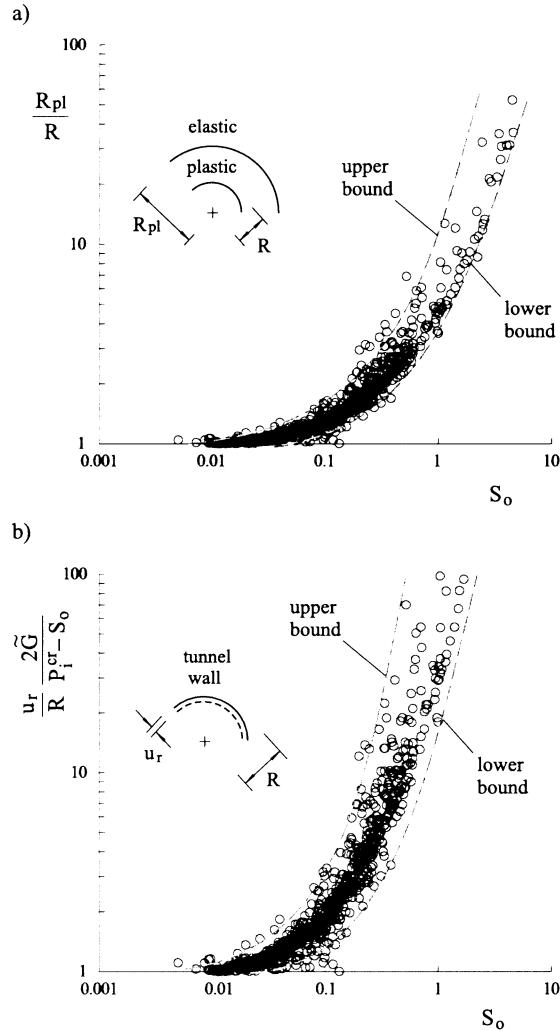


Figure 5. Graphical representation of the solution of 2,000 random tunnel cases (Figure 2) in terms of transformed stresses. a) Scaled extent of the failure region. b) Scaled radial displacement of the tunnel wall.

The numerical solution for the extent of the plastic zone and the radial convergence for each of the 2,000 cases will be determined using equations (23) and (28), respectively.

Figure 5 summarizes the results of the analysis. Figure 5a represents the scaled extent of the plastic zone R_{pl}/R as a function of the transformed far-field stress S_o —with S_o defined as in equations (13) or (16). Figure 5b represents the scaled extent of the radial displacement u_r at the wall of the tunnel also as a function of S_o . When the results of the randomly generated tunnel problems are presented in terms of transformed stresses, ‘order’ is introduced in the graphical representation of the (random in nature) results. In practical terms, this means that the solution can be bounded by upper and lower limits (e.g. as defined by the dotted curves in Figures 5), so that one can predict graphically (or analytically, after a curve-fitting has been made) the interval in which the solution can be expected to fall.

The importance of being able to bound the solution as described above becomes more apparent when no closed-form solution exists for the problem analyzed, and one needs to resort to heavy-computation schemes (like numerical models) to solve the problem. In such cases, the solution of a few well-chosen cases will allow the shape and position of the curves bounding the solution to be defined.

5. DISCUSSION

The transformation rule proposed in this paper allows a neat solution of the problem of excavating a circular tunnel subjected to uniform loading in generalized Hoek-Brown material to be obtained. Dimensionless representation of randomly generated tunnel cases computed with this solution shows that generality can be easily accomplished in the interpretation of results —also with the possibility of extrapolating results to other cases that are not actually solved.

The transformation rule proposed here can also be applied to analyze other cases for which no closed-form solution exists —such as tunnels with non-circular geometries or tunnels excavated in media subject to non-uniform loading. As explained in Section 4, numerical methods in combination with the proposed rule will allow definition of the fundamental relationships between input parameters and results, and the prediction of lower and upper limits for results obtained with the solution.

6. REFERENCES

- Brown, E. T., Bray, J. W., Ladanyi, B. & Hoek, E. 1983. Ground response curves for rock tunnels. *ASCE J. Geotech. Eng. Div.* 109(1), 15–39.
- Carranza-Torres, C. & Fairhurst, C. 1999. The elasto-plastic response of underground excavations in rock masses that satisfy the Hoek-Brown failure criterion. *International Journal of Rock Mechanics and Mining Sciences* 36(6), 777–809.
- Cundall, P., Carranza-Torres, C. & Hart, R. 2003. A new constitutive model based on the hoek-brown failure criterion. In Itasca Consulting Group Inc. (Ed.), *Proceedings of the Third International FLAC Symposium. "FLAC and Numerical Modeling in Geomechanics"*, Sudbury, Canada. October 21 to 24, 2003. Balkema.
- Hoek, E. & Brown, E. T. 1980. *Underground Excavations in Rock*. London: The Institute of Mining and Metallurgy.
- Hoek, E. & Brown, E. T. 1997. Practical estimates of rock mass strength. *International Journal of Rock Mechanics and Mining Sciences* 34(8), 1165–1186.
- Hoek, E., Carranza-Torres, C. & Corkum, B. 2002. Hoek-Brown failure criterion – 2002 edition. In R. Hammah, W. Bawden, J. Curran, & M. Telesnicki (Eds.), *Proceedings of NARMS-TAC 2002, Mining Innovation and Technology. Toronto – 10 July 2002*, pp. 267–273. University of Toronto.
- Hoek, E., Kaiser, P. K. & Bawden, W. F. 1995. *Support of Underground Excavations in Hard Rock*. Rotterdam: Balkema.
- Hoek, E., Marinos, P. & Benissi, M. 1998. Applicability of the Geological Strength Index (GSI) classification for very weak and sheared rock masses. The case of the Athens Schist Formation. *Bull. Eng. Geol. Env.* 57(2), 151–160.
- Itasca Consulting Group, Inc. 2000. *FLAC (Fast Lagrangian Analysis of Continua) Version 4.0*. www.itascacg.com, Minneapolis.
- Londe, P. 1988. Discussion on the determination of the shear stress failure in rock masses. *ASCE J. Geotech. Eng. Div.* 114(3), 374–376.
- Marinos, P. & Hoek, E. 2000. GSI: A geologically friendly tool for rock mass strength estimation. In *Proceedings of GeoEng2000, An International Conference on Geological and Geotechnical Engineering. November 2000, Melbourne, Australia*.
- Press, W. H., Flannery, B. P., Teukolsky, S. A. & Vetterling, W. T. 1994. *Numerical Recipes in C. The art of scientific computing* (Second ed.). New York: Cambridge University Press.
- Rocscience 2002. *Roclab. A freeware program for analysis of shear strength of rock according to the Hoek-Brown failure criterion*. www.roscience.com, Toronto.
- Serafim, J. L. & Pereira, J. P. 1983. Consideration of the geomechanical classification of Bieniawski. In *Proc. Int. Symp. on Engineering Geology and Underground Construction. Lisbon*, Volume 1(II), pp. 33–44.
- Sharan, S. K. 2003. Elastic-brittle-plastic analysis of circular openings in Hoek-Brown media. *International Journal of Rock Mechanics and Mining Sciences* 40(6), 817–824.
- Sofianos, A. I. 2003. Tunnelling Mohr-Coulomb strength parameters for rock masses satisfying the generalized Hoek-Brown failure criterion. *International Journal of Rock Mechanics and Mining Sciences* 40(3), 435–440.
- Wang, Y. 1996. Ground response of a circular tunnel in poorly consolidated rock. *ASCE J. Geotech. Eng.* 122(9), 703–708.

APPENDIX A: COMPARISON OF ANALYTICAL AND NUMERICAL (FLAC) RESULTS

The example presented here has been used to validate the implementation of a modified version of the generalized Hoek-Brown failure criterion in the finite difference code *FLAC* (Cundall, Carranza-Torres, & Hart 2003).

The problem considers the circular tunnel represented in Figure 2 and a generalized Hoek-Brown material characterized by two failure envelopes (Figure 4). The following are the variables defining the problem:

$$\begin{array}{lll}
R = 2 \text{ m} & \sigma_{ci} = 30 \text{ MPa} & \tilde{\sigma}_{ci} = 25 \text{ MPa} \\
p_i = 2.5 \text{ MPa} & m_b = 1.7 & \tilde{m}_b = 0.85 \\
\sigma_o = 15 \text{ MPa} & s = 3.9 \times 10^{-3} & \tilde{s} = 1.9 \times 10^{-3} \\
E = 5.7 \text{ GPa} & a = 0.55 & \tilde{a} = 0.60 \\
\nu = 0.3 & &
\end{array}$$

The numerical solution of the problem above was obtained with the spreadsheet described in Appendix B.

The results are represented in Figures A.1a and A.1b. Figure A.1a shows the distribution of radial and hoop stresses around the tunnel. Figure A.1b shows the corresponding distribution of radial displacements.

Good agreement is found between the analytical and the numerical *FLAC* results.

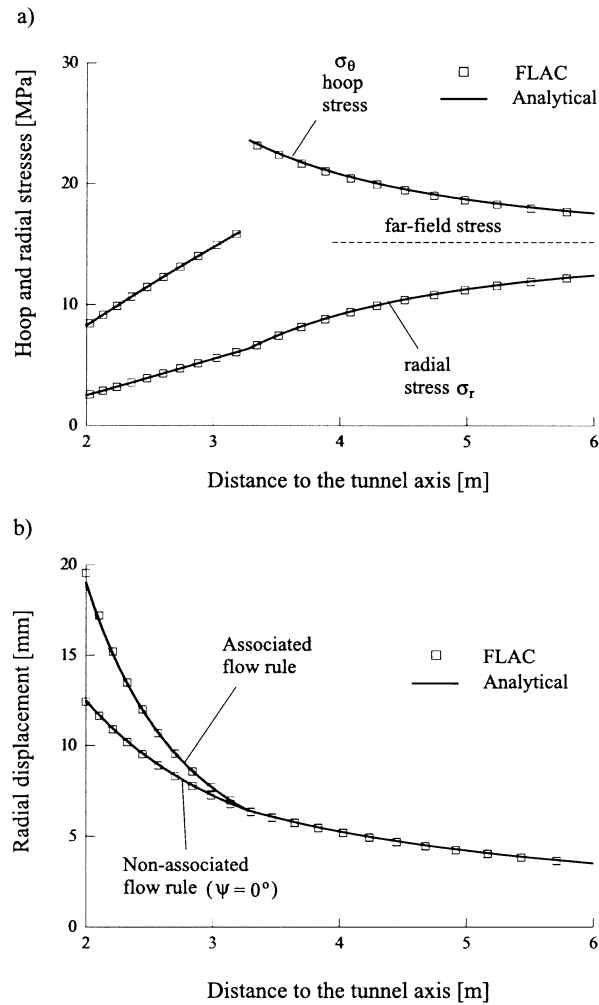


Figure A.1. Comparison of analytical and numerical *FLAC* results for the tunnel problem in Figure 2. a) Radial and hoop stresses. b) Radial displacements for associated and non-associated flow rules.

APPENDIX B: SPREADSHEET FOR THE IMPLEMENTATION OF THE TUNNEL SOLUTION

Figure B.2 shows the spreadsheet implementing the solution of the problem in Figure 2, according to the formulation discussed in Section 3 (the numerical values correspond to the example discussed in Appendix A).

The formulae in the different cells of the spreadsheet in Figure B.2 are listed in Figure B.3 (a copy of the electronic version of this Excel spreadsheet can be obtained by writing to the author at the address indicated on the first page).

The spreadsheet uses the 'solver' tool in Excel to obtain the solution of the transformed critical internal pressure (equation 20). To compute the solution, the user runs the solver for the input properties specifying the following parameters: *i*) 'Set Target Cell:' condition; *ii*) 'Value Of:' 0; *iii*) 'By Changing Cells:' piCR.

In the spreadsheet of Figure B.2, the differential equation (28) is integrated using the Runge-Kutta method (Press, Flannery, Teukolsky, & Vetterling 1994). The formulation is briefly outlined below.

Let us consider the following ordinary differential equation of second order,

$$u'' = U(\rho, u, u') \quad (\text{B.1})$$

In the equation above, ρ is the independent variable and u and u' are the unknown function and its first derivative, respectively.

Let us consider that the values of the function and its first derivative are known at ρ_1 —these will be denoted as u_1 and u'_1 , respectively.

The domain of integration is discretized into n zones of length h .

Starting with the boundary conditions u_1 and u'_1 at ρ_1 , the solution and its first derivative at every subsequent step $j + 1$ can be computed in terms of the solution in the previous step, j , according to the following expressions

$$u_{j+1} = u_j + h \left[u'_j + \frac{1}{6} (k_1 + k_2 + k_3) \right] \quad (\text{B.2})$$

$$u'_{j+1} = u'_j + \frac{1}{6} (k_1 + 2k_2 + 2k_3 + k_4) \quad (\text{B.3})$$

In the equations above, the coefficients k_1 , k_2 , k_3 and k_4 are computed as follows

$$k_1 = h \times U \left[\rho_j, u_j, u'_j \right] \quad (\text{B.4})$$

$$k_2 = h \times U \left[\rho_j + \frac{h}{2}, u_j + \frac{h}{2} u'_j, u'_j + \frac{h}{2} k_1 \right] \quad (B.5)$$

$$k_3 = h \times U \left[\rho_j + \frac{h}{2}, u_j + \frac{h}{2} u'_j + \frac{h^2}{4} k_1, u'_j + \frac{h}{2} k_2 \right] \quad (B.6)$$

$$k_4 = h \times U \left[\rho_j + h, u_j + h u'_j + \frac{h^2}{2} k_2, u'_j + h k_3 \right] \quad (B.7)$$

Equations (B.2) through (B.7) are implemented in the spreadsheet of Figure B.2 by the formulae listed in Figure B.3.

Spreadsheet for the computation of stress and displacement distributions around circular openings subject to symmetrical loading in generalized Hoek-Brown materials

(a) INPUT

(a1) Opening radius
R [m]: 2 (radius)

(a2) Loading
sig0 [MPa]: 15 (sig0)
pi [MPa]: 2.5 (pi)

(a3) Material properties

Deformability
E [MPa]: 5700.00 (young)
nu: 0.30 (poiss)
psi [deg]: 0.00 (psi)

Peak strength

sci: 30.00 (sci)
mb: 1.7000 (mb)
s: 3.90E-03 (s)
a: 0.5500 (a)

Residual strength

sciR: 25.00 (sciR)
mbR: 0.8500 (mbR)
sR: 1.90E-03 (sR)
aR: 0.6000 (aR)

(a4) Maximum radial distance (to plot results)

Rmax [m]: 10 (Rmax)

(b) OUTPUT

(b1) Intermediate computations

G [MPa]: 2192.31 (shear)
Kpsi: 1 (Kpsi)
A1: -1 (coeff_A1)
A2: 0.4 (coeff_A2)
A3: -0.4 (coeff_A3)

(b2) Critical internal pressure

Condition: 0.0000 (condition)
piCR [MPa]: 6.3785 (piCR)

(b3) Extent of plastic zone

Rpl [m]: 3.2794 (Rpl)

(b4) Boundary conditions

ur1 [m]: 0.006448 (ur1)
ur1P [m]: -0.008602 (ur1P)

(b6) Solution for the plastic region

h:	-0.0205 (c_h)					
point	r [m]	rho	sigr [MPa]	sigt [MPa]	k1	k2
1	3.2794	1.0000	6.3785	16.4231	0.0239	0.0245
2	3.2120	0.9795	6.1722	16.0222	0.0251	0.0257
3	3.1447	0.9589	5.9656	15.6182	0.0264	0.0271
4	3.0774	0.9384	5.7588	15.2112	0.0278	0.0286
5	3.0100	0.9179	5.5519	14.8011	0.0293	0.0302
6	2.9427	0.8973	5.3450	14.3879	0.0310	0.0319
7	2.8754	0.8768	5.1381	13.9715	0.0329	0.0339
8	2.8080	0.8563	4.9313	13.5520	0.0349	0.0360
9	2.7407	0.8357	4.7247	13.1293	0.0371	0.0383
10	2.6734	0.8152	4.5184	12.7034	0.0396	0.0409
11	2.6060	0.7947	4.3124	12.2743	0.0423	0.0437
12	2.5387	0.7741	4.1070	11.8420	0.0452	0.0468
13	2.4714	0.7536	3.9021	11.4065	0.0486	0.0503
14	2.4040	0.7331	3.6981	10.9678	0.0522	0.0542
15	2.3367	0.7125	3.4949	10.5260	0.0564	0.0586
16	2.2693	0.6920	3.2929	10.0812	0.0610	0.0635
17	2.2020	0.6715	3.0922	9.6333	0.0662	0.0690
18	2.1347	0.6509	2.8929	9.1824	0.0721	0.0752
19	2.0673	0.6304	2.6955	8.7287	0.0787	0.0823
20	2.0000	0.6099	2.5000	8.2723	0.0863	0.0904
(pt_P)	(r_P)	(rho_P)	(sigr_P)	(sigt_P)	(c_k1)	(c_k2)

(b5) Solution for the elastic region

point	r [m]	rho	sigr [MPa]	sigt [MPa]	ur [m]
1	10.0000	3.0494	14.0728	15.9272	0.0021
2	9.6463	2.9415	14.0036	15.9964	0.0022
3	9.2926	2.8336	13.9263	16.0737	0.0023
4	8.9388	2.7258	13.8396	16.1604	0.0024
5	8.5851	2.6179	13.7420	16.2580	0.0025
6	8.2314	2.5101	13.6316	16.3684	0.0026
7	7.8777	2.4022	13.5059	16.4941	0.0027
8	7.5240	2.2943	13.3622	16.6378	0.0028
9	7.1703	2.1865	13.1966	16.8034	0.0029
10	6.8165	2.0786	13.0046	16.9954	0.0031
11	6.4628	1.9707	12.7802	17.2198	0.0033
12	6.1091	1.8629	12.5157	17.4843	0.0035
13	5.7554	1.7550	12.2009	17.7991	0.0037
14	5.4017	1.6472	11.8223	18.1777	0.0039
15	5.0480	1.5393	11.3614	18.6386	0.0042
16	4.6942	1.4314	10.7924	19.2076	0.0045
17	4.3405	1.3236	10.0787	19.9213	0.0049
18	3.9868	1.2157	9.1667	20.8333	0.0053
19	3.6331	1.1079	7.9756	22.0244	0.0058
20	3.2794	1.0000	6.3785	23.6215	0.0064
(pt_E)	(r_E)	(rho_E)	(sigr_E)	(sigt_E)	(ur_E)

point	r [m]	rho	k3	k4	urP [m]	ur [m]
1	3.2794	1.0000	0.0245	0.0251	-0.0086	0.0064
2	3.2120	0.9795	0.0257	0.0264	-0.0091	0.0068
3	3.1447	0.9589	0.0271	0.0278	-0.0096	0.0068
4	3.0774	0.9384	0.0286	0.0293	-0.0102	0.0070
5	3.0100	0.9179	0.0302	0.0310	-0.0108	0.0072
6	2.9427	0.8973	0.0319	0.0329	-0.0114	0.0075
7	2.8754	0.8768	0.0339	0.0349	-0.0121	0.0077
8	2.8080	0.8563	0.0360	0.0371	-0.0127	0.0080
9	2.7407	0.8357	0.0383	0.0396	-0.0135	0.0082
10	2.6734	0.8152	0.0409	0.0423	-0.0143	0.0085
11	2.6060	0.7947	0.0437	0.0452	-0.0151	0.0088
12	2.5387	0.7741	0.0469	0.0486	-0.0160	0.0091
13	2.4714	0.7536	0.0504	0.0522	-0.0170	0.0095
14	2.4040	0.7331	0.0543	0.0564	-0.0180	0.0098
15	2.3367	0.7125	0.0586	0.0610	-0.0191	0.0102
16	2.2693	0.6920	0.0635	0.0662	-0.0203	0.0106
17	2.2020	0.6715	0.0691	0.0721	-0.0216	0.0111
18	2.1347	0.6509	0.0753	0.0787	-0.0230	0.0115
19	2.0673	0.6304	0.0824	0.0863	-0.0246	0.0120
20	2.0000	0.6099	0.0905	0.0949	-0.0263	0.0125
(pt_P)	(r_P)	(rho_P)	(c_k3)	(c_k4)	(urP_P)	(ur_P)

Figure B.2. Spreadsheet implementing the solution presented in Section 3. The numerical values correspond to the example described in Appendix A.

```

shear=young/2/(1+poiss)
Kpsi=(1+SIN(psi*PI()/180))/(1-SIN(psi*PI()/180))
coeff_A1=-Kpsi
coeff_A2=1-poiss-poiss*Kpsi
coeff_A3=poiss-(1-poiss)*Kpsi
condition=2*piCR+sci*(mb*piCR/sci+s)^a-2*sig0
Rpl=radius*EXP(((piCR/mbR^((1-a)/aR)/sciR+sR/mbR^(1/aR))
^(1-aR)-(pi/mbR^((1-aR)/aR)/sciR+sR/mbR^(1/aR))
^(1-aR)))/((1-aR)*mbR^((2*aR-1)/aR)))
ur1=Rpl/(2*shear)*(sig0-piCR)
ur1P=coeff_A1*ur1+Rpl/(2*shear)*(1-poiss*(1-coeff_A1))
*(piCR-sig0)-Rpl/(2*shear)*(coeff_A1+poiss
*(1-coeff_A1))*((piCR-sig0)+sciR*(mbR*piCR/sciR+sR)^aR)
pt_E=(filled with series 1 through 20)
r_E=Rmax-(pt_E-1)/(20-1)*(Rmax-Rpl)
rho_E=r_E/Rpl
sigr_E=sig0-(sig0-piCR)/rho_E^2
sigt_E=sig0+(sig0-piCR)/rho_E^2
ur_E=ur1/rho_E
pt_P=(filled with series 1 through 20)
r_P=Rpl-(pt_P-1)/(20-1)*(Rpl-radius)
rho_P=r_P/Rpl
sigr_P=((piCR/mbR^((1-aR)/aR)/sciR+sR/mbR^(1/aR))^(1-aR)
+(1-aR)*mbR^((2*aR-1)/aR)*LN(rho_P))^((1-aR))*sciR
*mbR^((1-aR)/aR)-(sR*sciR)/mbR
sigt_P=sigr_P+sciR*(mbR*sigr_P/sciR+sR)^aR
c_k1=coeff_A1/rho_P*ur_P-coeff_A1/rho_P^2*ur_P
+Rpl/(2*shear)*(coeff_A2*((piCR/mbR^((1-aR)/aR)/sciR
+sR/mbR^(1/aR))^(1-aR)+(1-aR)*mbR^((2*aR-1)/aR)
*LN(rho_P))^((aR/(1-aR))*sciR*mbR/(rho_P))-coeff_A3
*(sciR*mbR/(rho_P))*((piCR/mbR^((1-aR)/aR)/sciR
+sR/mbR^(1/aR))^(1-aR)+(1-aR)*mbR^((2*aR-1)/aR)
*LN(rho_P))^((2*aR-1)/(1-aR))*((piCR/mbR^((1-aR)/aR)
/sciR+sR/mbR^(1/aR))^(1-aR)+(1-aR)*mbR^((2*aR-1)/aR)
*LN(rho_P)+aR*mbR^((2*aR-1)/(aR))))))
c_k2=coeff_A1/(rho_P+c_h/2)*(ur_P+ur_P*c_h/2*c_k1)
-coeff_A1/(rho_P+c_h/2)^2*(ur_P+ur_P*c_h/2)+Rpl
/(2*shear)*(coeff_A2*((piCR/mbR^((1-aR)/aR)/sciR
+sR/mbR^(1/aR))^(1-aR)+(1-aR)*mbR^((2*aR-1)/aR)
*LN(rho_P+c_h/2))^((aR/(1-aR))*sciR*mbR/(rho_P+c_h))-coeff_A3*(sciR
*mbR/(rho_P+c_h))*((piCR/mbR^((1-aR)/aR)/sciR+sR/mbR
^(1/aR))^(1-aR)+(1-aR)*mbR^((2*aR-1)/aR)*LN(rho_P+c_h)
^((2*aR-1)/(1-aR))*((piCR/mbR^((1-aR)/aR)/sciR+sR/mbR
^(1/aR))^(1-aR)+(1-aR)*mbR^((2*aR-1)/aR)*LN(rho_P+c_h)
+aR*mbR^((2*aR-1)/(aR))))))
urP_P(1st cell)=ur1P
urP_P(remaining cells)=urP_P(previous row)
+c_h/6*(c_k1(previous row)+2*c_k2(previous row)
+2*c_k3(previous row)+c_k4(previous row))
ur_P(1st cell)=ur1
ur_P(remaining cells)=ur_P(previous row)
+c_h*(urP_P(previous row)+c_h/6
*(c_k1(previous row)+c_k2(previous row)
+c_k3(previous row)))

```

Figure B.3. Formulae to be entered in the cells of the spreadsheet in Figure B.2.